MICROWAVE ATOM CHIP FOR SPIN-SPECIFIC ATOM INTERFEROMETRY

William Miyahira[1] and Seth Aubin (advisor)[1]

[1]Department of Physics, William & Mary, Williamsburg, VA 23187

Abstract

The integration of ultracold atoms into quantum sensing devices for space-based applications could enhance measurement sensitivity and improve existing and future NASA missions. We present research on the development of a novel atom chip for atom interferometric sensing of gravitational and inertial navigation forces. The interferometer is based on broadband spin-specific AC Zeeman (ACZ) traps. Using parallel microstrip transmission lines we produce an ACZ trap at 6.8 GHz (^{87}Rb hyperfine transition frequency) 109 μm above the chip surface with a depth of 15 μK. Axial trapping is accomplished using a microwave lattice based on the ACZ or AC Stark effect. The lattice can also be used to translate atoms along the microstrips to form an atom interferometer. Additionally we include a scheme for traditional DC Zeeman chip trapping for which we show design and simulation. We have also developed a novel tapered microstrip wedge interface for efficient coupling of microwaves onto the micro-fabricated atom chip microstrips and show simulation and prototype work. To generate the microwave signals used for ACZ trapping we have constructed a multi-channel source with precise digital phase control based on IQ modulation featuring 90 dBc phase noise (1 kHz offset) and $\pm$50 MHz scan range from 6.8 GHz.

Introduction

Since their experimental discovery in the mid-90's [1], ultracold atoms have been used to revolutionize the realm of precision measurements. Using a technique known as atom interferometry, matter waves (i.e. ultracold atoms) are coherently split along different paths before being recombined and interfering. If the paths differ in any way, for example through a gravitational gradient or a rotation, the atom interferometer (AI) will accrue a phase difference between the paths resulting in interference fringes when recombined. From these fringes we can back out the phase difference and obtain precise measurements of physical forces. For example, using a 10 m tall "drop tower" atom interferometer [2], measurements of the acceleration due to gravity were made with a precision of $\Delta g/g = 3\times10^{-11}$.

Integration of high precision AIs into a compact physics package for space-based applications requires the use of an atom chip. These chips are cm-scale in length and width and feature micro-fabricated wires for generating the magnetic fields used for trapping and manipulation of ultracold atoms. NASA's cold atom laboratory (CAL) has recently demonstrated the ability to produce Bose-Einstein condensates aboard the International Space Station [3], with future upgrades in the BEC-CAL [4] and Quantum Explorer [5] in development as a robust platform for pushing past Earth-based AI experiments.

Precision quantum sensors using chip-scale AIs have a braod range of applications for NASA missions. For example, the GRACE-FO mission [6] could benefit from improved resolution and precision in obtaining information on planetary mass distributions (in particular water) for improved understanding of climate change and could have impact on agriculture and weather predictions [7]. This gravitational mapping technique could also be employed on a rover for exploring subterranean planetary features. In a Sagnac configuration AIs can be used for precision sensing of rotations and accelerations for improved inertial spacecraft navigation [8,9] in GPS-denied environments.

The research in the Aubin Lab at the College of William & Mary aims to develop a novel atom chip using the AC Zeeman (ACZ) effect to generate spin-specific potentials for trapping and manipulating ultracold atoms for atom interferometry.

AC Zeeman Traps for AI

Implementing the ACZ effect on an atom chip has multiple benefits over the traditional DC Zeeman effect:

- The ACZ potential is **inherently spin-specific** in contrast to the DC Zeeman potential, allowing the selection of favorable atomic states to improve AI performance.
- We can **operate multiple independent traps simultaneously**, a key aspect to our AI schemes.
- ACZ traps can be **operated at arbitrary magnetic field** giving the ability to tune the field to suppress AI noise.
- Since the lifetime of hyperfine atomic states is much longer than the experimental time scale, there is **no spontaneous emission**, thus removing a source of decoherence.
- ACZ traps have theoretically been shown to **suppress potential roughness** resulting from imperfections in atom chip manufacturing [10].

A scheme for a spin-dependent AI is shown in Fig. 1. It can be imagined as a Mach-Zehnder interferometer where the ACZ effect acts as a "beam-splitter" for ultracold atoms. In this configuration, independent traps for two atomic spin states, $|\uparrow\rangle$ and $|\downarrow\rangle$, are initially overlapped before being coherently split spatially along different paths. During the separation, the atoms are subject to an external potential (i.e. a gravitational gradient) for a time ΔT. When the traps are recombined the AI phase, $\frac{\Delta E \times \Delta T}{\hbar}$, can be read out by measuring the population of atoms in each spin state, $N_\uparrow$ and $N_\downarrow$.

We have already demonstrated a proof-of-principle ACZ trap on our lab's current atom chip using RF frequencies of $\sim$20 MHz [11] to target intra-manifold Zeeman transitions within a hyperfine level. This forms a system of more than two levels resulting in the participation of many spin states, however, we can use microwave frequencies of $\sim$6.8 GHz (in ^{87}Rb) to target inter-manifold transitions between hyperfine levels to form an effective two-level system conducive for AI experiments. Our current atom chip is not designed to efficiently handle AC currents of that frequency, so a new chip must be developed to support spin-specific microwave ACZ traps for atom interferometry.

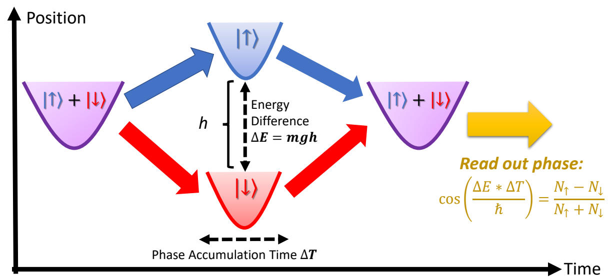

Figure 1: *Cartoon demonstrating an AI using ACZ traps. Initially, traps for the atomic states $|\uparrow\rangle$ and $|\downarrow\rangle$ are co-located before being coherently split spatially along two paths. In the presence of an external potential, i.e. gravity, there exists an energy difference, ΔE between the paths. After a time ΔT the traps are spatially recombined and the phase of the interferometer is read out to obtain ΔE.*

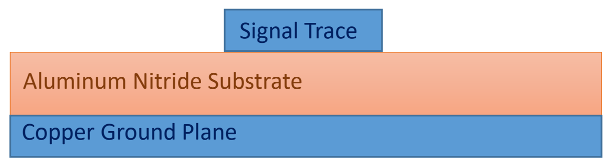

Figure 2: *Cross-section of the microstrip transmission line.*

This report is structured in the following manner. Section 1 describes the design and simulation of the microwave atom chip for ACZ trapping, as well as schemes for axial confinement and traditional DC chip trapping. Section 2 presents simulation and prototyping of a tapered microstrip wedge interface for efficiently coupling microwaves onto the atom chip. Section 3 shows the construction and testing of a multi-channel microwave source with precision phase control using IQ modulation. In section 4 we summarize the work presented and look forward to future research.

1 Atom Chip Development

The primary goal of this project is the development of an atom chip designed for performing AC Zeeman trapping and atom interferometry. The building block of the novel atom chip is the microstrip transmission line, a cross-section of which is shown in Fig. 2.

The microstrip consists of a copper ground plane

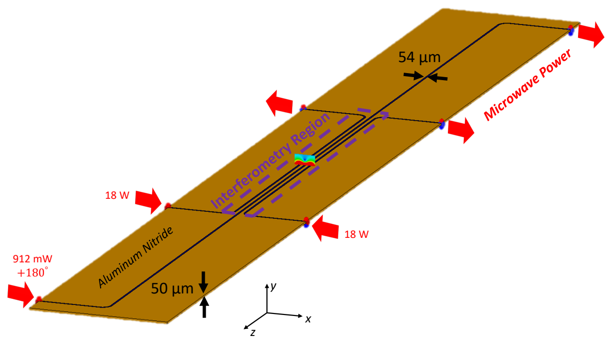

Figure 3: *CAD model of the microwave atom chip. The direction of microwave power in each microstrip along with the parameters used to generate the trap in Fig. 4 are indicated. The microstrips in the 1 cm long "interferometry region" are spaced 110 μm center-to-center. A slice of the simulated trap is shown in the center of the chip, which in reality spans the entire region.*

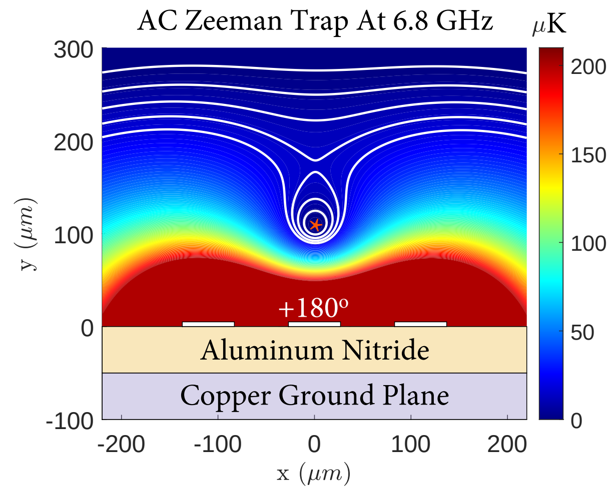

Figure 4: *Simulated ACZ potential using the chip design in Fig. 3. The potential uses a $2\pi\times1$ MHz and targets the $|2,2\rangle \leftrightarrow |1,1\rangle$ hyperfine transition in ^{87}Rb. Placing the current in the central microstrip (indicated by white rectangles) 180° out of phase with the outer microstrips the trap is formed 109 μm above the chip surface (red star). This produces a trap depth of 15 μK and a trap frequency of $2\pi\times426$ Hz. The white contours indicate curves of constant temperature and are placed every 5 μK.*

on top of which we put 50 μm of aluminum nitride (AlN). We choose to work with AlN because it has a relatively high dielectric constant (ϵ_r=8.9) which allows us to make narrow signal traces (roughly the substrate height, i.e. 50 μm) and a very high thermal conductivity (170 W/m$\times$K) allowing us to send large amounts of microwave power without breaking the microstrip. The microwave currents are carried in the signal trace, whose width is chosen such that the microstrip maintains a 50 Ω impedance for DC–20 GHz. From simulations we've found this is accomplished using a 54 μm trace width[12].

Our atom chip design is shown in Fig. 3. The central "interferometry region" consists of three parallel microstrips spaced 110 μm center-to-center. This region is 1 cm long and is where the interferometry experiments will take place. Using the electromagnetic simulation software FEKO we are able to simulate the magnetic field generated by sending microwaves through the chip traces. The resulting magnetic field in the x and y direction is shown at the center of the chip. We can turn this magnetic field into an ACZ potential as shown in Fig. 4. Notably, the microwave current in the central microstrip is 180° out-of-phase with the currents in the outer two traces. This generates a trap 109 μm above the chip surface (indicated by the red star in Fig. 4). Targeting the $|2,2\rangle \leftrightarrow |1,1\rangle$ hyperfine transition in ^{87}Rb with a detuning of $2\pi\times1$ MHz we simulate a trap depth of 15 μK and a radial trapping frequency of $2\pi\times426$ Hz.

Axial Trapping

The ACZ trapping scheme described in the previous section only confines atoms in the x and y directions, with nothing keeping them trapped axially along the traces. Without any axial trapping the ultracold atoms will leave through the ends of the interferometry region, thus nullifying any potential experiments. To provide axial confinement for the atoms we implement a microwave lattice (see Fig. 5). This is formed by sending counter-propagating microwave signals along a microstrips. When the microwaves interfere they form a standing wave that is stationary in time.

Another important aspect of the microwave lattice is that by adjusting the relative phase of the microwaves used to generate the lattice we are able to shift the position of the lattice axially along the microstrip trace. This is key for performing our interferometry scheme that relies on translating the two traps positionally along different paths. By separating the two traps such that they are centered on the two outer microstrips we can then use the lattice to move them axially for maximal arm separation.

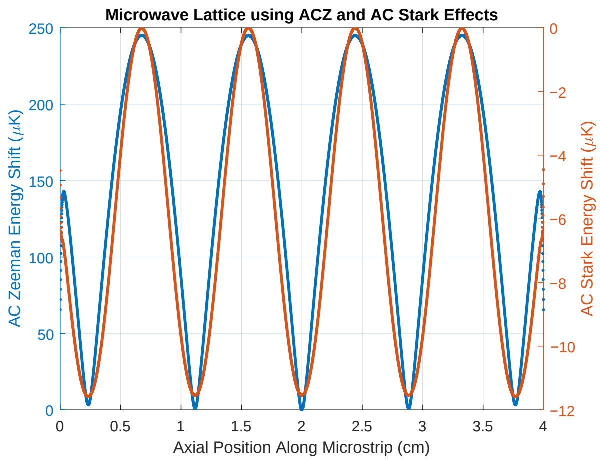

Figure 5: *Simulated ACZ (blue) and AC Stark (orange) lattice potentials produced by sending counter-propagating 12.5 W microwaves at 6.8 GHz along a single microstrip, evaluated 100 μm above the microstrip. The potential uses a detuning of $2\pi \times 1$ MHz and targets the $|2,2\rangle \leftrightarrow |1,1\rangle$ hyperfine transition in ^{87}Rb. Fig. adapted from Miyahira et. al.*[13]

AI Schemes

We show two practical AI schemes in Fig. 6 for gravimetry and Sagnac rotation sensing. Here, the independent $|\uparrow\rangle$ and $|\downarrow\rangle$ traps are initially overlapped above the center microstrip before being moved onto microwave lattices on the outer microstrips. Atoms can then be translated axially along the microstrips forming the different paths of the AI before being recombined.

DC Atom Chip Design

In addition to the ACZ portion of the chip, we also want to integrate a traditional DC Zeeman chip trap into our design. This allows us to perform initial trapping and cooling of atoms before transferring into the microwave AC trap, which is the procedure currently done in our RF ACZ trap[11]. In our design, we utilize the central z-shaped microstrip to perform trapping in the radial (x and y) direction, similar to our current DC atom chip trap. However, since the central portion of the z-trace is relatively long, the natural endcapping from the two end portions of the z-trace is not as strong, resulting in no axial (z direction) trapping. As shown in Fig. 7, we work around this by placing endcap wires below the main AC chip to provide axial trapping. To find working parameters for experiments, we can approximate the endcap wires as ideal 2D wires (since the trap loca-

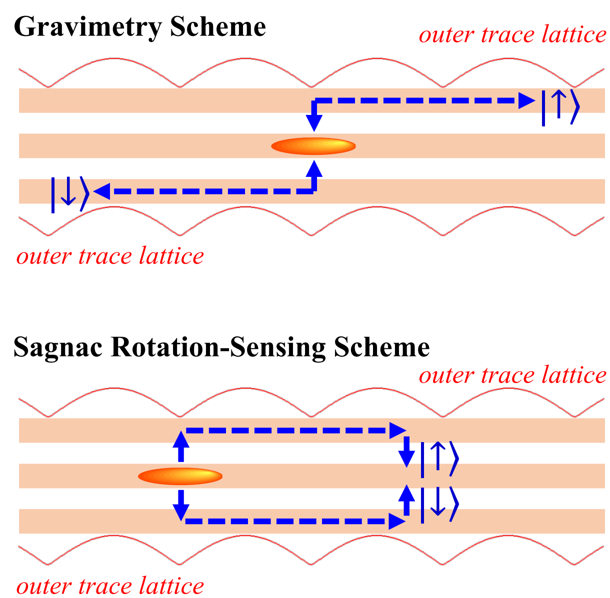

Figure 6: *AI schemes for a gravimetry (top) and Sagnac rotation sensing (bottoms) using spin-dependent ACZ traps. Axial translation along the traces is done using microwave lattices.*

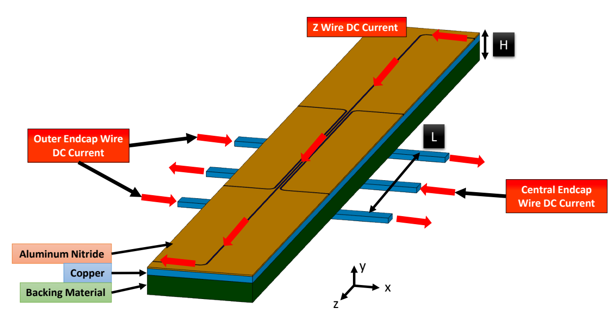

Figure 7: FEKO *model of the microwave atom chip operating in a traditional DC trapping scheme (not to scale). DC current is sent through the central Z-shaped microstrip for radial (x and y) trapping, while wires beneath the chip provide axial (z) confinement.*

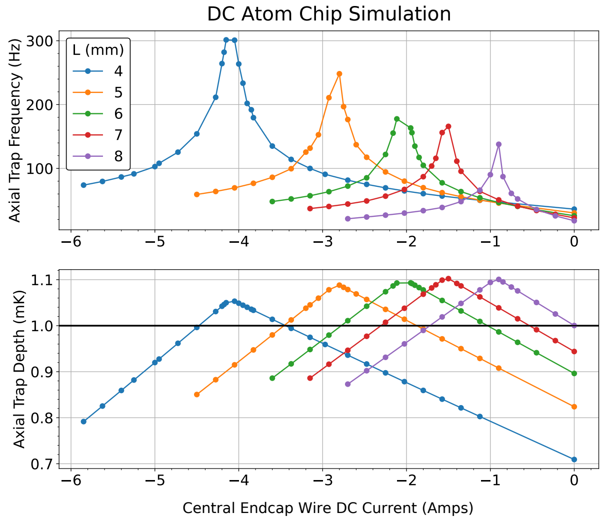

Figure 8: *Simulated axial trap frequencies and depths for H = 1 mm and 9 Amps in the outer endcap wires. The simulation shows results for different values of L across a range of central endcap wire currents.*

tion above the wires is much larger than the wire width). The trap features of interest are the trap depth and trap frequency. Our current DC atom chip features an axial trap frequency of 54 Hz and a trap depth of around 1 mK[14]. In designing the new DC part of the microwave atom chip, we would like to obtain similar trap parameters to ensure a viable DC trap.

We observe from simulation that we are able to achieve viable axial trap frequencies and depths for various endcap wire spacings. For the final chip design we intend on placing multiple endcap wires below the chip at various spacings, L, as shown in Fig. 8.

Eddy Current Measurements

One of the key design considerations in building atom chips is the presence of eddy currents in conducting materials in the system. These arise when DC currents in the atom chip traces are turned off, resulting in a changing magnetic field. From Maxwell's equations of electromagnetism, a time-varying magnetic field can induce an electric field, and generate currents, in a conductor in an effort to oppose the changing magnetic field. For the microwave atom chip, the microstrip groundplane is a layer of copper, which would be a source of eddy currents. To characterize how these eddy currents decay over time we placed a current carrying wire below a conducting material of known thickness. When the current in the wire is turned off eddy current will be induced in the conducting sample. We then use a magnetic field sensor (AKM EQ-730L Linear Hall Effect IC) to measure the decay time of the field generated by the induced eddy currents. From these tests we were able to find relationships between the material thickness and the eddy current decay time. We determine that thicknesses of less than 1 mm will work best for our experiments, corresponding to a decay time of less than 0.5 ms for high conductivity copper. Notably the double sided aluminum nitride samples offer low decay times as well as the mechanical strength needed for further atom chip manufacturing procedures. We are currently exploring using these samples as the main structure of the atom chip that the microstrips will be fabricated on.

2 Tapered Microstrip Wedge Interface

One of the primary engineering challenges faced when designing the microwave atom chip is being able to connect a standard SMA cable (mm diameter center conductor) to the microstrip chip traces (tens of microns wide). Being able to efficiently couple broadband signals (DC up to $\sim$20 GHz) allows for AC Zeeman trapping, a microwave lattice, and traditional DC chip trapping. The SMA-to-chip interface also needs to be compact (to fit in our current ultrahigh vacuum chamber) and easy to implement into the chip.

To resolve this engineering challenge we have come up with the tapered microstrip wedge interface, shown in Fig. 10. This design features a microstrip trace that tapers in width from about 1 mm (the size of an SMA cable) down to the 54 μm microstrips on the atom chip. To maintain 50 Ω impedance over the entirety of the wedge we simultaneously taper the aluminum nitride substrate height. We have progressed this in two areas: 1) Simulation using realistic chip parameters, and 2) Large-scale prototyping on Rogers 4350b substrate.

Simulation

To perform the simulation we utilize the electromagnetic simulation software HFSS. The simulation model and relevant parameters are shown in

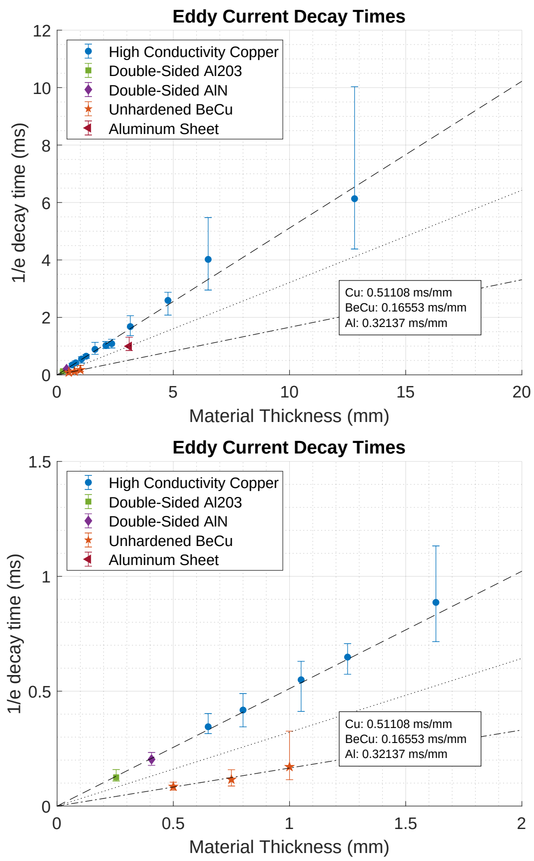

Figure 9: *(Top) Measured eddy current decay times for various materials and material thicknesses. (Bottom) Zoomed in plot showing decay times for low material thicknesses. Error bars in the measurements show the spread in decay times for six measurements (five for the double-sided substrates) at different magnetic field sensor heights. Linear fits were performed to obtain a relation between the thickness and decay time.*

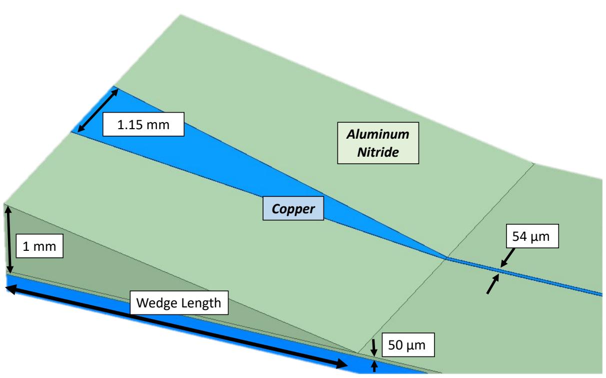

Figure 10: HFSS *model of the tapered microstrip wedge interface with relevant chip parameters. This model transitions from a 1.15 mm wide microstrip to the 54 µm wide atom chip traces.*

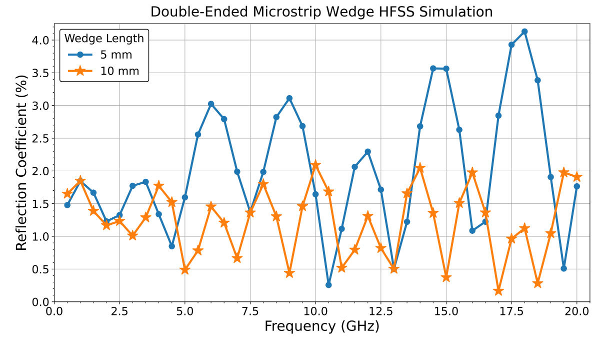

Figure 11: *Simulation of the tapered microstrip wedge interface using the parameters in Fig. 10 showing the reflection coefficient as a function of frequency. Results for a 5 mm and 10 mm long wedge are shown.*

Fig. 10. The results of the simulation are shown in Fig. 11, showing the reflection coefficient for a frequency range of 500 MHz to 20 GHz. We simulate two lengths of the wedge and demonstrate that the tapered microstrip wedge maintains under 4 % reflection for the entirety of the simulated frequency range.

Prototype Results

Prior to microfabricating the tapered microstrip wedge using the atom chip trace sizes we designed and built large scale prototypes using Rogers 4350b as the substrate. This tapers the microstrip trace from 3.7 mm to 1.75 mm. Using a vector network analyzer we are able to measure the impedance of the tapered microstrip wedge circuit out to 20 GHz, shown in Fig. 12. We observe that the wedge circuit maintains an impedance of 50 $\Omega \pm 10\ \Omega$ out to 9 GHz, which determines the usable bandwidth. While this does not extend to 20 GHz, it is well past our target frequency of 6.8 GHz for ACZ trapping of ^{87}Rb. We note that this bandwidth could be improved with better manufacturing of the wedges, as our in-house tapered substrates featured fractured traces at the end of the taper and imperfect substrate tapering.

3 Microwave Source

A necessity for doing AC Zeeman trapping on a chip is being able to precisely control the relative phase between neighboring microstrips. The phase can control features such as the trap location, strength, and near-field polarization. Additionally, when using a microwave lattice for axial trapping, chang-

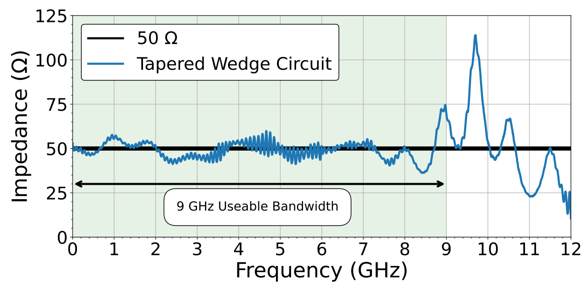

Figure 12: *Tests of the 1 cm long tapered microstrip wedge interface using a large-scale microstrip on Rogers 4350b substrate. Shown is the impedance for three double-ended wedge circuits and a microstrip with no wedges.*

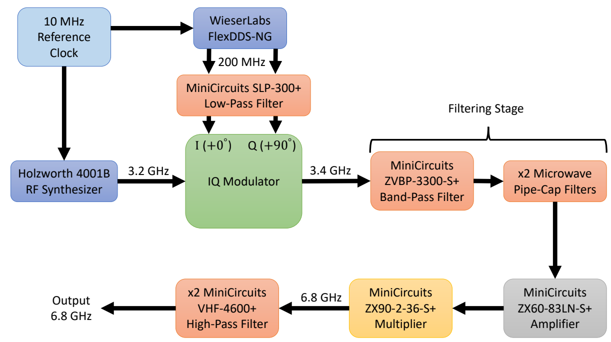

Figure 13: *Functional block diagram of one of the channels of the precision phase control microwave source.*

ing the phase difference between the signals generating the lattice will translate trapped atoms along the chip traces. This scheme can be configured for a number of atom interferometry schemes, such as for gravimetry or in a Sagnac interferometer for rotation sensing. For working with ^{87}Rb atoms, the frequency difference between the F=1 and F=2 ground state hyperfine manifolds is $\sim$6.8 GHz. In addition to being able to generate signals at this frequency, we also require a decently broad sweeping range (tens of MHz in each direction) for preparing atoms in the AC Zeeman states.

We have developed a microwave source at 6.8 GHz based on IQ modulation that allows for precise digital phase control with 50 MHz of scanable frequency range in each direction. A functional block diagram of a single channel is shown in Fig. 13. We employ a Holzworth 4001B ultra low phase-noise source as the local oscillator at 3.2 GHz which we modulate in frequency and phase with a 200 MHz signal from the WieserLabs FlexDDS-NG. The microwave pipe cap filters follow the design in the paper by Chen et. al.[15] to suppress the leakage of the local oscillator through the IQ modulator . Spectra of the 6.8 GHz output are shown in Fig. 14 with a span of 250 MHz and 10 kHz, respectively.

To demonstrate the ability to control the phase difference between channels we send two channels into a mixer. When the two inputs are at the same frequency the output of the mixer is a DC voltage. The value of the mixer output depends on the relative phase difference between the inputs and follows

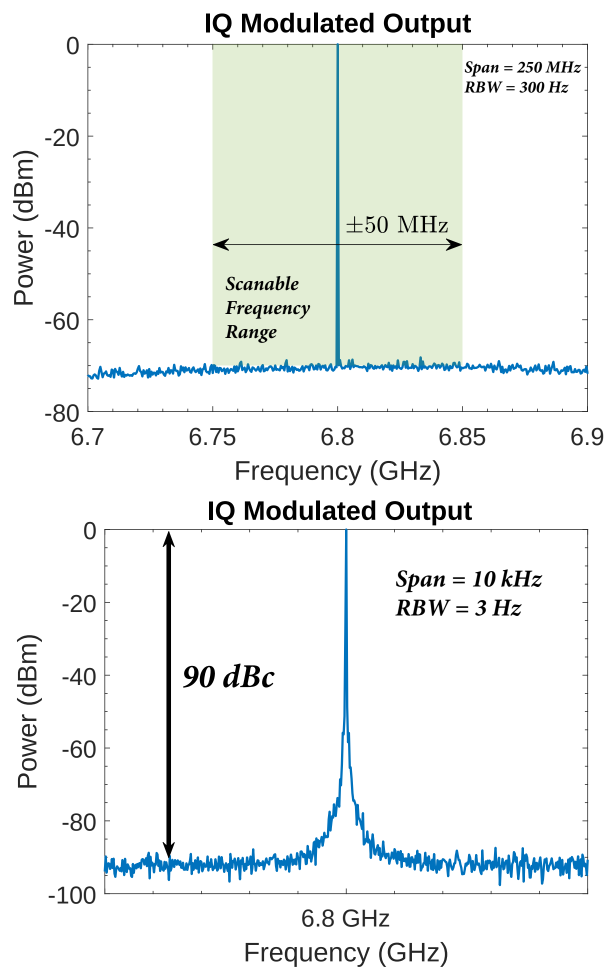

Figure 14: *Spectra of the iq modulated output at 6.8 GHz. (Top) 250 MHz span using a 300 Hz resolution bandwidth (RBW), highlighting the $\pm$50 MHz scan range. (Bottom) Close in spectrum with a 10 kHz span and 3 Hz RBW, with a phase noise of 90 dBc.*

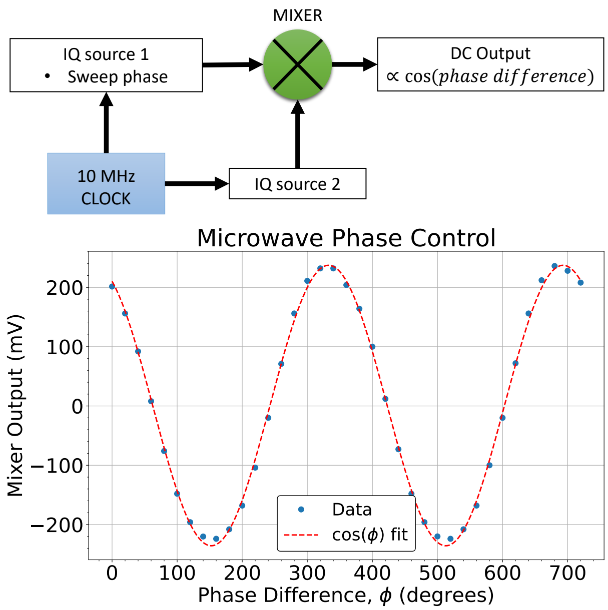

Figure 15: *(Top) Setup for testing control over relative phase between IQ modulated sources. With both sources synced to the same 10 MHz reference clock we sweep the phase of source 1 with respect to source 2. We then send both 6.8 GHz signals into a mixer which outputs a DC voltage proportional to the cosine of the phase difference between channels. (Bottom) Results showing relative phase control at 6.8 GHz. The blue points are data from the output of the mixer taken every 20° for a cycle of 4π. The red dashed curve shows a cosine fit.*

the relation

$$\text{Mixer Output } \propto \cos(\phi) \qquad (1)$$

where ϕ is the relative phase difference between microwave channels. Following this procedure we can map out the DC output from the mixer as a function of the phase difference between channels as seen in Fig. 15.

4 Conclusion and Future Work

We have presented design and simulation of a novel atom chip utilizing parallel microstrip transmission lines for spin-specific microwave ACZ trapping of ultracold atoms for atom interferometry. To efficiently couple broadband microwave signals onto the micro-fabricated atom chip we show simulation and prototype work of a tapered microstrip wedge interface used to focus microwaves from coaxial cables with mm-scale field modes down to the 54 μm microstrips. We generate microwave signals with precise relative phase control for trapping using IQ modulation of an ultra-low phase noise source.

Moving forward, the majority of the lab's research will focus on the manufacturing of the microwave atom chip and implementing it into our ultracold atom apparatus for AI experiments. With the simulation and prototypes of the tapered microstrip wedge interface showing promising results for broadband operation we will be working to make tapered wedges on aluminum nitride with trace sizes compatible with the atom chip (i.e. those shown in Fig. 10). To perform the microfabrication of the atom chip and tapered microstrip wedge interfaces we are working with the group of Professor Vitaly Avrutin at Virginia Commonwealth University. Once the final chips have been completed we will integrate it into our existing apparatus for testing and characterization before moving onto initial atom interferometry experiments.

Acknowledgments

WHM is supported by the Virginia Space Grant Consortium (VSGC), NSF Grant # 1806558, DTRA Grant # HDTRA1-19-1-0027, with partial funding from a VMEC Seed Grant from ARL. We would also like to acknowledge collaborations with Professor Vitaly Avrutin, David Pate, and Trevor Tingle at Virginia Commonwealth University (VCU) as well as with the teams at Nitride Global and Kadco Ceramics.

References

[1] Mike H Anderson, Jason R Ensher, Michael R Matthews, Carl E Wieman, and Eric A Cornell. Observation of bose-einstein condensation in a dilute atomic vapor. *Science*, 269(5221):198–201, 1995.

[2] Susannah M Dickerson, Jason M Hogan, Alex Sugarbaker, David MS Johnson, and Mark A Kasevich. Multiaxis inertial sensing with long-time point source atom interferometry. *Physical review letters*, 111(8):083001, 2013.

[3] David C Aveline, Jason R Williams, Ethan R Elliott, Chelsea Dutenhoffer, James R Kellogg, James M Kohel, Norman E Lay, Kamal Oudrhiri, Robert F Shotwell, Nan Yu, et al. Observation of bose–einstein condensates in an earth-orbiting research lab. *Nature*, 582(7811):193–197, 2020.

[4] Kai Frye, Sven Abend, Wolfgang Bartosch, Ahmad Bawamia, Dennis Becker, Holger Blume, Claus Braxmaier, Sheng-Wey Chiow, Maxim A Efremov, Wolfgang Ertmer, et al. The bose-einstein condensate and cold atom laboratory. *EPJ Quantum Technology*, 8(1):1, 2021.

[5] RJ Thompson, D Aveline, SW Chiow, ER Elliott, JR Kellogg, J m Kohel, MS Sbroscia, L Phillips, C Schneider, JR Williams, et al. Exploring the quantum world with a third generation ultra-cold atom facility. *Quantum Science and Technology*, 8(1):014007, 2022.

[6] Frank Webb, Frank Fletchtner, Felix Landerer, Phil Morton, Michael Watkins, Himanshu Save, Christoph Dahle, Srinivas Bettadpur, Robert Gaston, and Michael Gross. Gravity recovery and climate experiment follow-on mission. 2019.

[7] Rainer Kaltenbaek, Antonio Acin, Laszlo Bacsardi, Paolo Bianco, Philippe Bouyer, Eleni Diamanti, Christoph Marquardt, Yasser Omar, Valerio Pruneri, Ernst Rasel, et al. Quantum technologies in space. *Experimental Astronomy*, 51(3):1677–1694, 2021.

[8] B Barrett, A Bertoldi, and P Bouyer. Inertial quantum sensors using light and matter. *Physica Scripta*, 91(5):053006, 2016.

[9] I Dutta, D Savoie, B Fang, B Venon, CL Garrido Alzar, R Geiger, and A Landragin. Continuous cold-atom inertial sensor with 1 nrad/sec rotation stability. *Physical review letters*, 116(18):183003, 2016.

[10] S Du, AR Ziltz, W Miyahira, and S Aubin. Suppression of potential roughness in atom-chip ac zeeman traps. *Physical Review A*, 105(5):053127, 2022.

[11] Andrew Rotunno. *Radiofrequency AC Zeeman Trapping for Neutral Atoms*. PhD thesis, College of William & Mary, 2021.

[12] Shuangli Du. *AC and DC Zeeman interferometric sensing with ultracold trapped atoms on a chip*. PhD thesis, College of William & Mary, 2021.

[13] William Miyahira, Andrew P Rotunno, ShuangLi Du, and Seth Aubin. Microwave atom chip design. *Atoms*, 9(3):54, 2021.

[14] MK Ivory, AR Ziltz, CT Fancher, AJ Pyle, A Sensharma, B Chase, JP Field, A Garcia, D Jervis, and S Aubin. Atom chip apparatus for experiments with ultracold rubidium and potassium gases. *Review of Scientific Instruments*, 85(4):043102, 2014.

[15] Zilong Chen, Justin G Bohnet, Joshua M Weiner, and James K Thompson. A low phase noise microwave source for atomic spin squeezing experiments in 87rb. *Review of Scientific Instruments*, 83(4):044701, 2012.